12-1990

Quantum Invariants: Topographical Map of Quantized Actions

Niraj Srivastava
University of Rhode Island

Gerhard Müller
University of Rhode Island, gmuller@uri.edu

Citation/Publisher Attribution
N. Srivastava and G. Müller. *Quantum invariants: topographical map of quantized actions*. Comments At. Mol. Phys. 25 (1990), 59-65.
Available at: http://www.worldcat.org/title/comments-on-atomic-and-molecular-physics/oclc/813488

Quantum Invariants: Topographical Map of Quantized Actions

Niraj Srivastava [1] and Gerhard Müller [1]

[1] Department of Physics, University of Rhode Island, Kingston RI 02881, USA

For Hamiltonian systems with two degres of freedom, quantum invariants as constructed via time averages of dynamical variables in energy eigenstates provide a convenient representation of quantum nonintegrability effects in the form of a topographical map of quantized actions.

Quantum chaos stands at the junction of two major developments in physics which have taken place during the past decade:

- the realization by the physics community at large that deterministic chaos in dynamical systems with few degrees of freedom is of paradigmatic significance, and that its ramifications for the dynamics of microscopic physical systems are of fundamental importance;
- the enormous refinement of experimental techniques in atomic and molecular physics, now allowing for extremely detailed studies of the dynamics of real quantum systems with few degrees of freedom
- to illuminate the still obscure connection between (i) classical Hamiltonian chaos defined as deterministic randomness and (ii) quantum nonintegrability effects identified and analyzed in quantum model systems;
- to establish a firm and transparent connection between (ii) evident quantum nonintegrability effects and (iii) experimental results for specific dynamical properties of real quantum few-body systems.

At present the pivotal links (i) $\leftrightarrow$ (ii) $\leftrightarrow$ (iii) are fairly indirect for the most part, dictated by matters of practicality. The most convenient formulation used for the description of items (i), (ii), (iii) are often sufficiently different to invite some degree of ambiguity in interpretation. Under these circumstance it is imperative that the exploration of new representations for the study of quantum nonintegrability effects be continued vigorously for the purpose of more direct comparisons.

One such representation, which turns out to be quite useful and illuminating for the analysis of quantum manifestations of Hamiltonian chaos in systems with two degrees of freedom, is the topographical map of quantized actions in the form of quantum invariants. In the following, we give a brief description and illustration of this representation for a system consisting of two exchange-coupled spins with biaxial exchange and single-site anisotropy,

$$\hat{H} = \hbar^2 \sum_{\mu=xyz} \left\{ -J_\mu \hat{\sigma}_1^\mu \hat{\sigma}_2^\mu + \frac{1}{2} A_\mu \left[\left(\hat{\sigma}_1^\mu\right)^2 + \left(\hat{\sigma}_2^\mu\right)^2 \right] \right\}. \tag{1}$$

It defines, in the limit $\hbar \to 0$, $\sigma \to \infty$, $\hbar\sqrt{\sigma(\sigma+1)} = s$, $\hbar\hat{\sigma}_l^\mu = S_l^\mu$, an autonomous classical Hamiltonian system $H(\mathbf{S}_1, \mathbf{S}_2)$ with two degrees of freedom for a pair of 3-component vectors $\mathbf{S}_l$ of length s. The classical integrability condition is nontrivial, $(A_x - A_y)(A_y - A_z)(A_z - A_x) + J_x^2(A_y - A_z) + J_y^2(A_z - A_x) + J_z^2(A_x - A_y) = 0$ and a 2nd integral of them motion $I(\mathbf{S}_1, \mathbf{S}_2)$ is explicitly known for the integrable cases [1,2].

Integrability of the classical 2-spin cluster implies that the flow in four-dimensinal (4d) phase space is confined to 2d tori. The phase space is densely foliated by such tori. Each torus is specified by the values of two action variables J_1, J_2, and the two independent analytic invariants are functions of these two action variables: $H(\mathbf{S}_1, \mathbf{S}_2) = E(J_1, J_2)$, $I(\mathbf{S}_1, \mathbf{S}_2) = I'(J_1, J_2)$. The corresponding quantum energy spectrum E_λ is then naturally catalogued as a two-parameter family in terms of quantum numbers m_1, m_2, $-\sigma, -\sigma+1, \ldots, \sigma$, $k = 1, 2$ in accordance with semiclassical quantization.

This implicit 2d order of the eigenvalue sequence E_λ in terms of the two quantized action variables can be displayed even if the function $E(J_1, J_2)$ is not explicitly known. Consider the energy eigenvalues E_λ and the eigenvalues I_λ of the quantum invariant $\hat{I}$, the quantum version of $I(\mathbf{S}_1, \mathbf{S}_2)$. In a diagram I_λ versus E_λ, the 2d array of points then forms a regular pattern, a fully intact 2d web with four bonds per vertex. This invariant-web is likely to be visually distorted due to the generally complicated nonlinear dependence of E and I' on J_1, J_2.

The main plot of Fig. 1 shows such an invariant-web. There we have plotted the eigenvalues $I_\lambda^{(M)}$ of the second invariant $\hat{I}_M$ (to be specified) versus the eigenvalues E_λ for an integrable case of the 2-spin model (1) (see caption for specification). The vertices represent all eigenvalues $E_\lambda > 0$ of the states (for $\sigma = 35$) which transform according to the irreducible representations A1A or

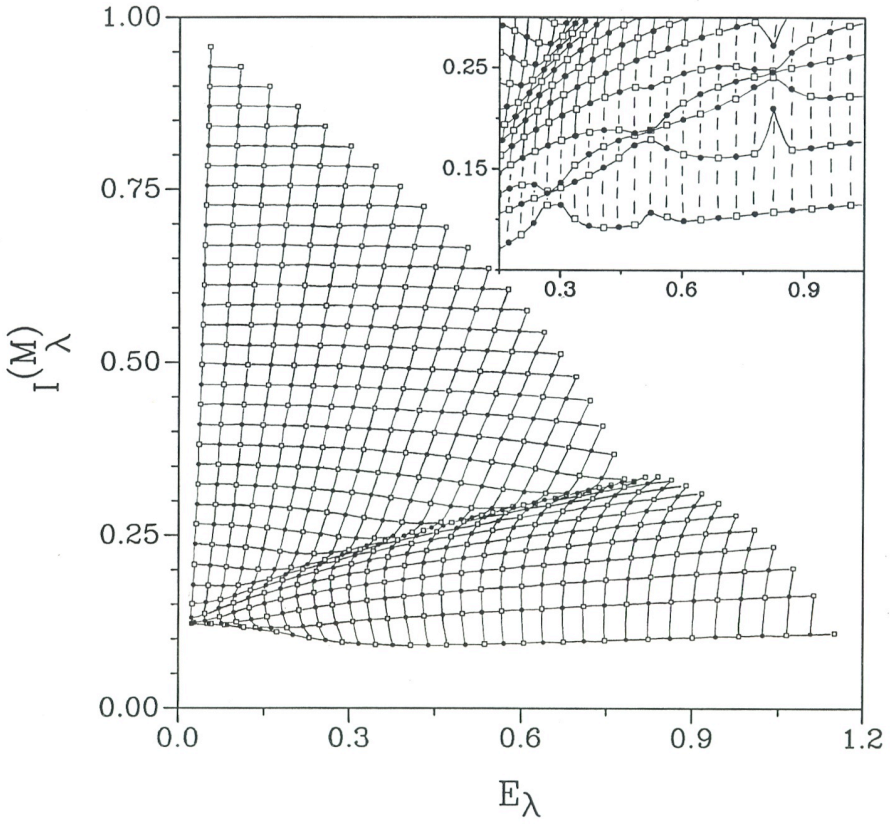

Figure 1. Quantum invariant $I_\lambda^{(M)}$ versus energy E_λ for all eigenstates (with $E_\lambda > 0$) of symmetry classes A1A (full circles) and B1S (open squares) of the integrable case $J_x = 1.2, J_y = 0.8, J_z = 0, A_x = A_y = A_z = 0$ of the quantum 2-spin model (1) for $s = 1$ and spin quantum number $\sigma = 35$. The inset shows the same quantities for the nonintegrabe case $J_x = J_y = 1, J_z = 0, A_x = -A_y = -0.4, A_z = 0$ of Hamiltonian (1), but only for quantum states within a window of given size in the $(E_\lambda, I_\lambda^{(M)})$-plane.

B1S of the symmetry group $D_2 \otimes S_2$, where S_2 is the permutation group of the two spins and D_2 contains all twofold rotations about the coordinate axes [3].

In the action plane, each quantized torus claims a square of area $\hbar^2$, in accordance with the uncertainty principle. Those squares map onto the meshes of the invariant-web. The threads of the web can be interpreted as lines of constant action and the meshes along one such line as incremental marks in units of *hbar* for the other action variable. Note that one set of threads change from positive to negative slope going through a point of infinite slope if the quantum states are smoothly interpolated. Interpreting this set of threads as lines of constant J_2, it follows that one of two fundamental frequencies of the classical time evolution, $\omega_1 = \partial E(J_1, J_2)/\partial J_1$, slows down to zero at the point of infinite slope, which signals the presence of a separatrix in the action plane. All this is suggestive of the name "topographical map of quantized actions," which we have given to this representation of quantum invariants.

We could have constructed our 2nd invariant $\hat{I}$ directly from the classical integral of the motion as derived in Ref. 1. Instead, following an idea of Peres [4], we construct $\hat{I}$ from some arbitrary dynamical variable via time average: Take any dynamical variable $\hat{A}$ which is independent of $\hat{H}$ (e.g. choose $\hat{A}$ such that $[\hat{A}, \hat{H}] \neq 0$), and consider the matrix elements of $\hat{A}(t)$ in the energy representaion, $\langle\lambda|\hat{A}(t)|\lambda'\rangle = \langle\lambda|\hat{A}|\lambda'\rangle \exp[(E_\lambda - E_{\lambda'})t/\hbar]$. Performing the time average eliminates all off-diagonal elements and thus defines the quantum invariant $\hat{I}_A$, which is diagonal in the energy representation as it should be: $\overline{\langle\lambda|\hat{A}(t)|\lambda'\rangle} = \langle\lambda|\hat{A}|\lambda'\rangle\delta_{\lambda\lambda'} \equiv I_\lambda^{(A)}\delta_{\lambda\lambda'}$. In the case where degenerate energy levels occur, the eigenvectors in the invariant subspaces must be chosen such that all off-diagonal elements $\langle\lambda|\hat{A}|\lambda'\rangle$ are zero.

Throughout this study we use the quantum invariant $I_\lambda^{(M)} = \sqrt{\langle\lambda|\hat{M}_z^2|\lambda\rangle}$ with $\hat{M}_z = \hbar(\hat{\sigma}_1^z + \hat{\sigma}_2^z)/2$, which is, for the integrable cases of (1), a valid substitute for the invariant operators derived from the explicitly known classical analytic invariant $I(\mathbf{S}_1, \mathbf{S}_2)$. The fully intact web in Fig. 1 illustrates this situation. However, $I_\lambda^{(M)}$ can also be constructed for nonintegrable cases of (1), cases for which the classical analytic invariant $I(\mathbf{S}_1, \mathbf{S}_2)$ does not exist. Not surprisingly, the properties of $I_\lambda^{(M)}$ depend sensitively on whether the classical integrability condition is satisfied or not.

Figure 1 shows in juxtaposition the characteristic properties of quantum invariants in the vicinity of a separatrix for an integrable model (main plot) and a near-integrable model (inset). The two models (see caption for specifications) have exactly the same symmetries. A distinctive feature of the nonintegrable case is that nearly degenerate states (of the same symmetry class) tend to resonate in the vicinity of the separatrix line, which in this case is the quantum image of a narrow chaotic band in phase space. Several such resonances – some strong, some weak – can be observed in the inset to Fig. 1.

If we change the model parameters such as to generate a wider band of chaos along the separatrix in the classical phase flow, more and more resonances make their appearance in the associated quantum invariant-web. As the number of resonances increases, they begin to overlap. This situation is illustrated in the web depicted in the main plot of Fig. 2. The overlap of resonances was introduced by Chirikov [5] as a criterion for widespread chaos in the context of classical perturbation theory, and quantum analogs of that concept have since been used in a number of different applications [6].

The inset to Fig. 2 shows a situation in which the chaotic band along the classical separatrix is so wide as to cause the complete disintegration of the corresponding quantum invariant-web. No individual resonances can be identified any more. Within the chaotic region, the quantum states now tend to cluster in short strips along lines which interpolate one set of threads across the chaotic separatrix line, leaving sizable areas of th $(E_\lambda, I_\lambda^{(M)})$-plane almost depleted of states. Within any one of these small clusters, the quantum states are slightly displaced sideways, enough to account for the effect of level repulsion after projection on to the E_λ-axis [7].

Note that classical Hamiltonian chaos, even though it is dense everywhere in phase space, does not manifest itself in quantum mechanics as long as the chaotic regions are small compared to the mesh size of the quantum-invariant web. This describes the situation in the two regular regions on both sides of the separatrix in Fig. 2.

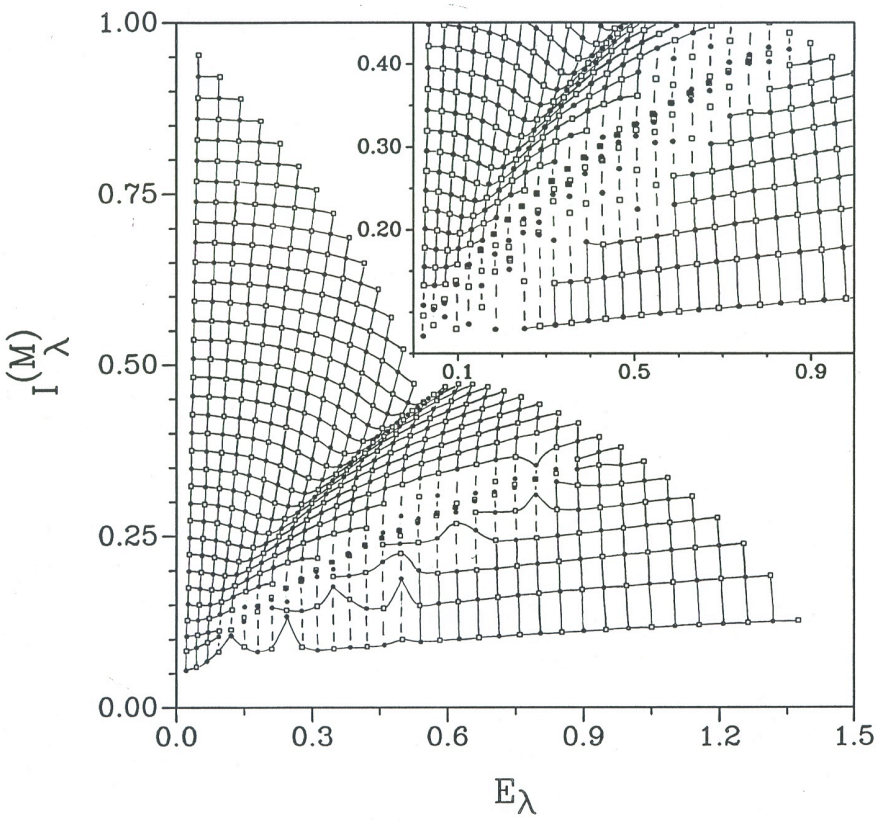

Figure 2. Quantum invariant $I_\lambda^{(M)}$ versus energy E_λ for all eigenstates (with $E_\lambda > 0$) of symmetry classes A1A (full circles) and B1S (open squares) of the nonintegrable case $J_x = J_y = 1, J_z = 0, A_x = -A_y = -0.45, A_z = 0$ of the quantum 2-spin model (1) for $s = 1$ and spin quantum number $\sigma = 35$. The inset shows the same quantities for the case $J_x = J_y = 1, J_z = 0, A_x = -A_y = -0.5, A_z = 0$ of the same model but only for quantum states within a window of given size in the $(E_\lambda, I_\lambda^{(M)})$-plane.

In summary, the topographical map of quantized actions as obtained from quantum invariants is a convenient representation for the study of integrable and nonintegrable Hamiltonian systems with two degrees of freedom. It provides unmistakable quantum images of the most conspicuous phenomena of classical Hamiltonian chaos such as resonances between nonlinear modes and the breakdown of invariant tori in the classical phase flow.

Acknowledgment: This work was supported in part by the U.S. National Science Foundation Grant DMR-86-03036 and by Sigma Xi. the Scientific Research Society. The numerical calculations were performed on the CRAY-2 of the National Center for Supercomputing Applications, University of lllinois at Urbana-Champaign. We have used a modified cmpj.sty style file.

References

1. E. Magyari, H. Thomas, R. Weber, C. Kaufman and G. Müller, Z. Phys. B **65** ,363 (1987).
2. N. Srivastava, C. Kaufman, G. Müller, R. Weber and H. Thomas, Z. Phys. B **70**, 251 (1988).
3. P. W. Atkins, M. S. Child and C. S. G. Phillips, *Tables for Group Theory* (Oxford University Press, 1970).
4. A. Peres, Phys. Rev. Lett. **53**, 1711 (1984).

5. B. V. Chirikov, Phys. Rep. **52**, 263 (1979).
6. G. P. Berman, G. M. Zaslavskii and A. R. Kolovsky, Phys. Lett. **87A**, 152 (1982); W. A. Lin and L. E. Reichl, Phys. Rev. A **37**, 3972 (1988).
7. N. Srivastava, C. Kaufman, G. Müller. R. Weber and H. Thomas, J. Appl. Phys. (in press).